This is the Pre-Published Version.

This document is the Accepted Manuscript version of a Published Work that appeared in final form in ACS Applied Materials and Interfaces, copyright © American Chemical Society after peer review and technical editing by the publisher. To access the final edited and published work see https://dx.doi.org/10.1021/acsami.1c14505.

A passive fuel cell fed with an electrically rechargeable liquid fuel

Xingyi Shi[1], Yichen Dai[1], Oladapo Christopher Esan[1], Xiaoyu Huo[1], Liang An*[, 1], Tianshou Zhao*[, 2]

[1] Department of Mechanical Engineering, The Hong Kong Polytechnic University, Hung Hom, Kowloon, Hong Kong SAR, China

[2] Department of Mechanical and Aerospace Engineering, The Hong Kong University of Science and Technology, Clear Water Bay, Kowloon, Hong Kong SAR, China

* Corresponding authors.

Email: liang.an@polyu.edu.hk (L. An)

Email: metzhao@ust.hk (T.S. Zhao)

Abstract

Passive fuel cells, using diffusion and natural convection for fuel delivery, are regarded as promising candidates for powering portable devices including mobile phones and laptops. However, the performance of passive fuel cells which employ typical liquid alcohol fuels are still limited, which thereby greatly hampered their commercialization progress. Recently, a novel concept named the electrically rechargeable liquid fuel (e-fuel), with its rechargeability, cost-effectiveness, and superior reactivity, has attracted increasing attention. In this study, a passive fuel cell using the liquid e-fuel and the ambient air for electricity production is designed and fabricated. This passive fuel cell is demonstrated to achieve a peak power density of 116.2 mW cm^{-2} along with a stable operation for over 350 hours, exhibiting great prospect for future applications.

Keywords: E-fuel; Passive fuel cell; Current collector design; Power density; Long-term

stability; Hydrogen evolution

1. Introduction

As a result of the increasing needs of renewable energy, the development of sustainable power generation systems has become a major research direction and drawn world-wide attention. In comparison to other existing technologies, fuel cell technology has been acknowledged as a promising candidate and utilized in numerous applications including electric vehicles, mobile devices, and even power stations.[1-3] Among the various types of fuel cell, direct liquid fuel cells attributed to their high energy density and ease of fuel handling, have been extensively studied.[4-5] Nevertheless, to realize the commercialization of direct liquid fuel cells, especially in small devices such as mobile phones and laptops, it is necessary to minimize or completely eliminate auxiliary equipment such as pumps, air blowers, and heat controllers from the system.[6-8] Passive fuel cells, using diffusion and natural convection for fuel delivery, have therefore received extensive studies in recent years.[9-10] However, as a result of the slow reaction kinetics of conventional liquid fuels, poor performance, such as lower peak power density than the typical active liquid fuel cells, is a major limitation of these passive liquid fuel cells.[11-12] To boost the performances of passive liquid fuel cells, it is thus of paramount importance to explore alternative fuels with better reactivity.

Recently, a novel concept named the electrically rechargeable liquid fuel (e-fuel), which possesses many advantages such as rechargeability and superior reactivity over the conventional liquid alcohol fuels, was presented.[13-15] Potential liquid e-fuel can be prepared from diverse kinds of material and it has been reported in recent studies that the e-fuel containing vanadium ions is capable of achieving a better performance including much higher peak power density and energy efficiency than conventional direct liquid fuel cells do.[14-16]

Herein, drawn by the superiorities of the e-fuel, a passive fuel cell has been designed and fabricated utilizing the liquid e-fuel and paired with the ambient air for electricity production. This passive fuel cell using the liquid e-fuel impressively results in a peak power density of 116.2 mW cm^{-2} along with a stable operation for over 350 hours, which therefore place it as a promising candidate with great prospects to realize future applications.

2. Working principle

The passive fuel cell structure (**Figure 1**) includes a membrane electrode assembly (MEA), an e-fuel tank, a pair of current collectors and endplates. During the cell operation, the V^{2+} ions in the e-fuel are oxidized to V^{3+} ions at the anode side, while the oxygen reduction reaction (ORR) occurs at the cathode side. The overall reaction is thus given as:

$$V^{2+} + H^{+} + \frac{1}{4}O_2 \rightarrow V^{3+} + \frac{1}{2}H_2O \qquad \Delta E = 1.49\ V \qquad (1)$$

The theoretical voltage of this system is 1.49 V,[14] which is higher than those of many common direct alcohol fuel cells.

3. Experimental Section

3.1 Preparation of MEA

The MEA of this passive fuel cell (2.0 × 2.0 cm^2) was fabricated following the method reported previously,[14] where a thermally treated graphite felt and a Pt/C coated carbon paper (2.0 mg cm^{-2}) was used as anode and cathode, respectively.[14] Nafion 117 pretreated following the standard procedure reported previously was used as proton exchange membrane in the middle of the MEA.[14]

3.2 Cell assembly and experimental apparatus

The passive fuel cell system consisting of an e-fuel tank and a pair of current collectors and end plates was fabricated. The home-made e-fuel tank was prepared using acrylic with two holes drilled on its top for e-fuel injection. The e-fuel was prepared by first dissolving $VOSO_4$ into H_2SO_4 and thereafter charged by a typical flow cell. Deionized water was sprayed onto the cathode to pre-humidify the electrode surface while 20.0 mL e-fuel to be supplied into the cell was injected into the tank before further tests. Five current collectors (CCs) with different designs and open ratios (ORs) were fabricated using graphite, namely CC1 to CC5. Among them, CC1 and CC2 adopted the circular perforation design, while CC3 to CC5 adopted the rectangular parallel channels design.[9] The OR of each current collector from CC1 to CC5 is 25.97%, 28.27%, 35.00%, 50.00%, and 70.00%, respectively. In addition, a transparent fuel cell with an acrylic end plate and a graphite current collector engraved with a serpentine flow filed was also fabricated to enable the visualization of the gas evolution process at the anode. For the transparent fuel cell, a peristaltic pump was used for the e-fuel delivery at ~5.0 mL min^{-1}, while the cell is under open circuit condition during the test.

The polarization and long-term discharge tests were performed using an Arbin BT2000 (Arbin instrument Inc.). All experiments were conducted at ambient condition. For the long-term operation behavior test, the Faradic, voltage and energy efficiencies are calculated using the following equations[15]:

$$\text{Faradic efficiency } (\%) = \frac{\int i(t)dt}{c_{init}VF} \quad (1)$$

$$\text{Voltage efficiency } (\%) = \frac{E_{aver}}{E_{theo}} = \frac{E_{aver}}{\frac{\int_0^{c_{init}}[E^0 + \frac{RT}{F}\ln(\frac{c_{V2+}}{c_{V3+}})]dc}{c_{init}}} \quad (2)$$

$$\text{Energy efficiency } (\%) = \text{Faradic efficiency} \times \text{Voltage efficiency} \quad (3)$$

$i(t)$ is the discharging current, while c_{init} and V represents the initial concentration of e-fuel and volume of e-fuel, respectively. E_{aver} and $E_{theo}$is the average discharging voltage and theoretical average voltage calculated based on the Nernst equation, respectively.

4. Results and discussion

4.1 General performance of the passive fuel cell

The general performance of this developed passive fuel cell is as depicted in **Figure 2 (a)**, where the cell is assembled with CC5 and using an e-fuel of 1.0 M V^{2+} ions. The cell is found to achieve an open-circuit voltage (OCV) of 1.29 V with a peak power density of 116.2 mW cm^{-2}. It is worth to mention that, during the operation of this passive fuel cell, the V^{2+} ions would inevitably transport through the membrane to the cathode side, which thereby leads to a mixed potential due to the simultaneous oxygen reduction reaction and vanadium oxidation reaction and hence resulted in the potential loss.[14] However, when compared with the conventional passive and active liquid fuel cells reported before, as shown in **Figure 2 (b)** and **Table S1**, this passive fuel cell utilizing the e-fuel is found to demonstrate a much higher peak power density. Such an outstanding cell performance is ascribed to the superior reactivity of the e-fuel at room temperature along with the optimized current collector design which allows the ease of e-fuel delivery. Hence, it is considered that this passive fuel cell fed with the e-fuel possesses great potential for future applications.

4.2 Effect of the current collector design

As one of the main components of a passive fuel cell, the current collector (CC) plays multiple

roles during the cell operation, which include allowing the conduction of electrons between the electrode surface and the external circuit, and providing the pathways for the fuel delivery and products removal.[17] It is hence essential for the current collector to have superior electric conductivity and ease of fuel transport.[9] In this work, five CCs with various opening patterns and ratios are designed and fabricated to optimize the cell performance. As shown in **Figure 3 (a)**, CC1 and CC2 adopted the circular perforation design, while CCs 3-5 adopted the rectangular parallel channels design.[9] All the CCs are assembled into the passive fuel cell to conduct the polarization tests and the results are as presented in **Figure 3 (b)**. It can be seen that, feeding the cell with an e-fuel of 0.6 M V^{2+} ions, both the maximum current density and the peak power density of the cell raise with the increment of the CC open ratio. In addition, the concentration loss at the end of the polarization curve is found to decrease in this order. Such result is due to the fact that, a higher open ratio of CC can provide larger pathways for fuel supply, which thereby facilitate the transport of both oxygen and the e-fuel.[17] However, it is worth noticing that allowing a higher reactant contact area through a CC of high open ratio could on the other hand lead to a high interfacial ohmic loss due to the sacrificed electric contact area for electrons transport, which can eventually limit the cell performance.[17] Still, overall, CC5 with its highest open ratio achieved the best performance among all the CCs tested and is therefore chosen and used for further studies in this work.

4.3 Effect of the e-fuel concentration

As mentioned, the passive fuel cell only utilizes natural diffusion and convection for fuel delivery.[10] Hence, for a given cell design, the concentration of fuel in the tank is a major variable with significant influence on the mass transport of reactants and the availability of

sufficient reactants to the reactive surface, which is of paramount importance towards determining the cell performance.[18] Here, in order to examine the effects of the e-fuel concentration on the cell performance, the liquid e-fuel with V^{2+} ions concentration varying from 0.2 M to 1.0 M are studied. As shown in **Figure 3 (c)**, the activation and concentration losses of the cell are found to reduce effectively with the increase of e-fuel concentration. It is because the high concentration of reactive species can lead to a raise of the fuel concentration gradient between the tank and electrode surface, which thereby results in an enhanced mass transport.[18] This improved e-fuel delivery thereby can help to provide more reactive species to the anode and hence promote the e-fuel oxidation reaction, leading to a better cell performance. However, it should also be noted that the usage of e-fuel with higher concentration would on the other hand promote the crossover of V^{2+} ions through the membrane and thereby lead to the loss of fuel.[19] Furthermore, the permeated V^{2+} ions to the cathode side can also result in a mixed potential due to the simultaneous e-fuel oxidation and oxygen reduction reactions, which can further deteriorate the cell performance.[14, 20]

4.4 Long-term operation behavior

It is a crucial requirement for the passive fuel cell to attain a superior long-term stability before realizing its wide commercialization. Here, to study the long-term operation behavior of this system, the passive fuel cell has been tested at 5.0 mA cm^{-2} and refueled for 25 times. The discharge curves are as shown in **Figure 4 (a)**, while the associated efficiencies - Faradic, voltage, and energy efficiencies are calculated using the equations as reported before[15] and as shown in **Figure 4 (b)**. The cell is found to achieve a stable operation for over 350 hours, with little difference between the discharge curves obtained at the first and last cycle, indicating the

excellent long-term stability of this system. It is also found that, in comparison to the discharge curve obtained at the first cycle, the cell voltage at the last cycle is slightly lower. Such a phenomenon may be ascribed to the crossover of reactive species across the membrane inducing the accumulation of vanadium ions at the cathode side, which thereby block the reactive surface of the catalysts and enlarges overpotential loss.[14-15, 21] Furthermore, it is worth mentioning that, an unexpected gas evolution phenomenon was observed at the anode side during the test, which can also obstruct the reactive surface at the anode and hamper the mass transport of reactants, resulting in the fluctuation of cell voltage as demonstrated in the discharge curves.[22-23] This phenomenon is later proved as a spontaneous hydrogen evolution reaction and discussed extensively in the next section. Such a reaction accompanied with the inevitable crossover of e-fuel through the membrane would result in the loss of reactive species, which thereby lead to the loss of Faradic efficiency and further reduces the energy efficiency of the cell. Overall, this present passive cell is found to achieve a stable energy efficiency of ~40% during the 25 times of refueling tests, demonstrating its superior capability for long-term operation.

4.5 Visualizations of anode flow channels

As discussed in the previous section, during the long-term operation of this passive fuel cell, an unexpected gas evolution phenomenon is observed at its anode side, which limits the transport of the reactants and deteriorates the cell performance.[21] In order to further observe and examine this phenomenon, a transparent cell is designed and fabricated as shown in **Figure 5**, where a new graphite current collector engraved with a serpentine flow field is fabricated and used as the anode current collector while CC5 is used at the cathode side. This transparent

cell is assembled three times using the same MEA used for the previous tests, a used graphite felt, and a fresh graphite felt, respectively. Four different solutions, including 3.0 M H_2SO_4, and 1.0 M $VO^{2+}/V^{3+}/V^{2+}$ in 3.0 M H_2SO_4, are fed into the anode side of the cell and the results are as shown in **Figure S1**. Gas evolution was only observed when the e-fuel of 1.0 M V^{2+} is used (**Figure 6 (a)-(c)**), which thereby indicate the occurrence of a spontaneous gas evolution reaction.

Considering the superior reactivity of V^{2+} ions, even without any catalyst, the following reaction as reported before might have happened,[24-25] which results in a hydrogen generation process:

$$V^{2+} + H^{+} \rightarrow V^{3+} + \frac{1}{2}H_2 \quad (2)$$

To prove and justify this idea, the generated gas is then collected from the outlet of the transparent cell by water displacement method and then fed into a typical hydrogen-oxygen fuel cell, which results in an OCV of 1.11 V (**Figure S2**) similar to the value obtained when this cell is fed with pure hydrogen, thereby proving the presence of a spontaneous hydrogen evolution reaction (HER) at the anode side. It is worth to mention that, during the visulization tests, a similar gas evolution phenomenon is observed in the cell using the used MEA and the used graphite felt, while a less severe gas generation process is observed when the fresh thermally treated graphite felt anode is tested (**Figure 6(a)-(c)**).[24] Such a phenomenon is considered to be attributed to the superior catalytic reactivity of Pt, which penetrate from the cathode side across the membrane after the cell operation.[26-27] It is also worth to stress that, this spontaneous HER should be regarded with great importance in this passive fuel cell system as it could severely deteriorate the cell performance from the following aspects: i) the HER can

occupy the reactive surface on the anode and lead to large overpotential loss;[28] ii) this HER will consume the reactive species and lead to fuel capacity loss; and iii) the generated hydrogen gas can hamper the mass transport of the fuel and results in large mass transport polarization.[21] This HER may also raise safety concerns and thus requires careful attention. It is therefore a critical consideration to develop an electrode of good reactivity to the e-fuel oxidation reaction while suppressing the spontaneous HER so as to gain a better cell performance. In addition, it is also essential to prevent any potential contamination from the environment during the cell assembling and develop a membrane that can efficiently suppress the transport of catalyst from the cathode side so as to attain a more stable cell performance.

5. Summary

In this work, a passive fuel cell utilizing the liquid e-fuel and ambient air for power generation is designed and fabricated. It is found that both the current collector open ratios and e-fuel compositions show a major effect on the transport of reactant inside the cell, which thereby greatly influences the cell performance. The cell remarkably demonstrates a peak power density of 116.2 mW cm^{-2} along with a stable operation for over 350 hours, which even outperforms many conventional active liquid fuel cells. Such a superior performance therefore validates the capability of this developed passive fuel cell for wide-spread application in the future especially for powering mobile devices. However, it is also found that a spontaneous hydrogen evolution reaction happens at the anode, which would decrease the e-fuel capacity and further deteriorate the cell performance. It is thus believed that further performance enhancement of this passive fuel cell can be achieved in the future with the development of electrode with superior reactivity to the e-fuel while also suppressing the undesired hydrogen

evolution reaction. Water flooding, which is another critical issue responsible for limiting the performance of this passive fuel cell, also needs to be addressed as it can hamper the delivery of oxygen and thereby deteriorate the reaction kinetics at the cathode side. It is therefore essential to investigate the influences of water flooding on the cell performance and develop a suitable membrane and electrode to attain a better cell performance in the future.

Conflicts of interest

There are no conflicts to declare.

Supporting Information

The visualization photos of the anode flow channels with complete MEA, used and fresh thermally treated graphite felt anode while feeding different solutions/e-fuels; Voltage profile of the hydrogen-oxygen fuel cell fed with the generated gas from the anode side of the passive fuel cell; and Table with detailed comparison of power densities among various liquid fuel cells.

Acknowledgement

The work described in this paper was fully supported by a grant from the Research Grant Council of the Hong Kong Special Administrative Region, China (Project No. T23-601/17-R).

References

1. Wang, Y.-J.; Qiao, J.; Baker, R.; Zhang, J., Alkaline Polymer Electrolyte Membranes for Fuel Cell Applications. *Chemical Society Reviews* **2013,** *42* (13), 5768-5787.
2. Laberty-Robert, C.; Valle, K.; Pereira, F.; Sanchez, C., Design and Properties of Functional Hybrid Organic–Inorganic Membranes for Fuel Cells. *Chemical Society Reviews* **2011,** *40* (2), 961-1005.
3. Yuan, X.; Ding, X.-L.; Wang, C.-Y.; Ma, Z.-F., Use of Polypyrrole in Catalysts for Low Temperature Fuel Cells. *Energy & Environmental Science* **2013,** *6* (4), 1105-1124.
4. Antolini, E., Palladium in Fuel Cell Catalysis. *Energy & Environmental Science* **2009,** *2* (9), 915-931.
5. Tadanaga, K.; Furukawa, Y.; Hayashi, A.; Tatsumisago, M., Direct Ethanol Fuel Cell Using Hydrotalcite Clay as a Hydroxide Ion Conductive Electrolyte. *Advanced Materials* **2010,** *22* (39), 4401-4404.
6. Zhao, T.; Chen, R.; Yang, W.; Xu, C., Small Direct Methanol Fuel Cells with Passive Supply of Reactants. *Journal of Power Sources* **2009,** *191* (2), 185-202.
7. Pan, Z.; Bi, Y.; An, L., Performance Characteristics of a Passive Direct Ethylene Glycol Fuel Cell with Hydrogen Peroxide as Oxidant. *Applied Energy* **2019,** *250*, 846-854.
8. Oliveira, V.; Pereira, J.; Pinto, A., Modeling of Passive Direct Ethanol Fuel Cells. *Energy* **2017,** *133*, 652-665.
9. Mallick, R. K.; Thombre, S. B.; Shrivastava, N. K., A Critical Review of the Current Collector for Passive Direct Methanol Fuel Cells. *Journal of Power Sources* **2015,** *285*, 510-529.
10. Munjewar, S. S.; Thombre, S. B.; Mallick, R. K., Approaches to Overcome the Barrier Issues of Passive Direct Methanol Fuel Cell–Review. *Renewable and Sustainable Energy Reviews* **2017,** *67*, 1087-1104.
11. Wang, Z.; Zhang, X.; Nie, L.; Zhang, Y.; Liu, X., Elimination of Water Flooding of Cathode Current Collector of Micro Passive Direct Methanol Fuel Cell by Superhydrophilic Surface Treatment. *Applied Energy* **2014,** *126*, 107-112.
12. Munjewar, S. S.; Thombre, S. B.; Patil, A. P., Passive Direct Alcohol Fuel Cell Using Methanol and 2-Propanol Mixture as a Fuel. *Ionics* **2019,** *25* (5), 2231-2241.
13. Jiang, H.; Wei, L.; Fan, X.; Xu, J.; Shyy, W.; Zhao, T., A Novel Energy Storage System Incorporating Electrically Rechargeable Liquid Fuels as the Storage Medium. *Science Bulletin* **2019,** *64* (4), 270-280.
14. Shi, X.; Huo, X.; Ma, Y.; Pan, Z.; An, L., Energizing Fuel Cells with an Electrically Rechargeable Liquid Fuel. *Cell Reports Physical Science* **2020,** *1* (7), 100102.
15. Shi, X.; Huo, X.; Esan, O. C.; An, L.; Zhao, T., Performance Characteristics of a Liquid E-fuel Cell. *Applied Energy* **2021,** *297*, 117145.
16. Shi, X.; Huo, X.; Esan, O. C.; Ma, Y.; An, L.; Zhao, T., A Liquid E-fuel Cell Operating at −20° C. *Journal of Power Sources* **2021,** *506*, 230198.
17. Braz, B.; Moreira, C.; Oliveira, V.; Pinto, A., Effect of the Current Collector Design on the Performance of a Passive Direct Methanol Fuel Cell. *Electrochimica Acta* **2019,** *300*, 306-315.
18. Liu, J.; Zhao, T.; Chen, R.; Wong, C., The Effect of Methanol Concentration on the Performance of a Passive DMFC. *Electrochemistry Communications* **2005,** *7* (3), 288-294.

19. Hao, L.; Wang, Y.; He, Y., Modeling of Ion Crossover in an All-vanadium Redox Flow Battery with the Interfacial Effect at Membrane/Electrode Interfaces. *Journal of The Electrochemical Society* **2019,** *166* (8), A1310-A1322.
20. Pereira, J.; Falcão, D.; Oliveira, V.; Pinto, A., Performance of a Passive Direct Ethanol Fuel Cell. *Journal of Power Sources* **2014,** *256*, 14-19.
21. Wei, L.; Zhao, T.; Xu, Q.; Zhou, X.; Zhang, Z., In-situ Investigation of Hydrogen Evolution Behavior in Vanadium Redox Flow Batteries. *Applied Energy* **2017,** *190*, 1112-1118.
22. Noack, J.; Cognard, G.; Oral, M.; Küttinger, M.; Roznyatovskaya, N.; Pinkwart, K.; Tübke, J., Study of the Long-term Operation of a Vanadium/Oxygen Fuel Cell. *Journal of Power Sources* **2016,** *326*, 137-145.
23. Liu, B.; Li, Z.; Zhu, J.; Suda, S., Influences of Hydrogen Evolution on the Cell and Stack Performances of the Direct Borohydride Fuel Cell. *Journal of Power Sources* **2008,** *183* (1), 151-156.
24. Sun, C.-N.; Delnick, F. M.; Baggetto, L.; Veith, G. M.; Zawodzinski Jr, T. A., Hydrogen evolution at the negative electrode of the all-vanadium redox flow batteries. *Journal of Power Sources* **2014,** *248*, 560-564.
25. Peljo, P.; Vrubel, H.; Amstutz, V.; Pandard, J.; Morgado, J.; Santasalo-Aarnio, A.; Lloyd, D.; Gumy, F.; Dennison, C.; Toghill, K. E., All-vanadium dual circuit redox flow battery for renewable hydrogen generation and desulfurisation. *Green Chemistry* **2016,** *18* (6), 1785-1797.
26. Guilminot, E.; Corcella, A.; Charlot, F.; Maillard, F.; Chatenet, M., Detection of Pt z+ ions and Pt nanoparticles inside the membrane of a used PEMFC. *Journal of The Electrochemical Society* **2006,** *154* (1), B96.
27. Akita, T.; Taniguchi, A.; Maekawa, J.; Siroma, Z.; Tanaka, K.; Kohyama, M.; Yasuda, K., Analytical TEM study of Pt particle deposition in the proton-exchange membrane of a membrane-electrode-assembly. *Journal of Power Sources* **2006,** *159* (1), 461-467.
28. Chen, F.; Liu, J.; Chen, H.; Yan, C., Study on Hydrogen Evolution Reaction at a Graphite Electrode in the All-vanadium Redox Flow Battery. *Int. J. Electrochem. Sci* **2012,** *7* (4), 3750-3764.

Figure captions

Figure 1 (a) Working principle, (b) design, and (c) fabrication of a passive fuel cell.

Figure 2 (a) General performance of a passive fuel cell; (b) Comparison of the peak power density of the passive fuel cell with the data available in the open literature.

Figure 3 (a) Designs of five current collectors; (b) Polarization and power density curves of this passive fuel cell with different designs; and (c) Polarization and power density curves of this passive fuel cell with various e-fuel concentrations.

Figure 4 (a) Long-term discharging behavior and comparison of the 1st and 25th discharging curves of this passive fuel cell (insert). (b) The Faradic, voltage, and energy efficiencies of this passive fuel cell.

Figure 5 (a) Design and (b) fabrication of a fuel cell with a transparent anode flow field.

Figure 6 Visualizations of anode flow channels with (a) complete MEA, (b) used and (c) fresh thermally treated graphite felt anode, when fed with e-fuel (1.0 M V^{2+} in 3.0 M H_2SO_4).

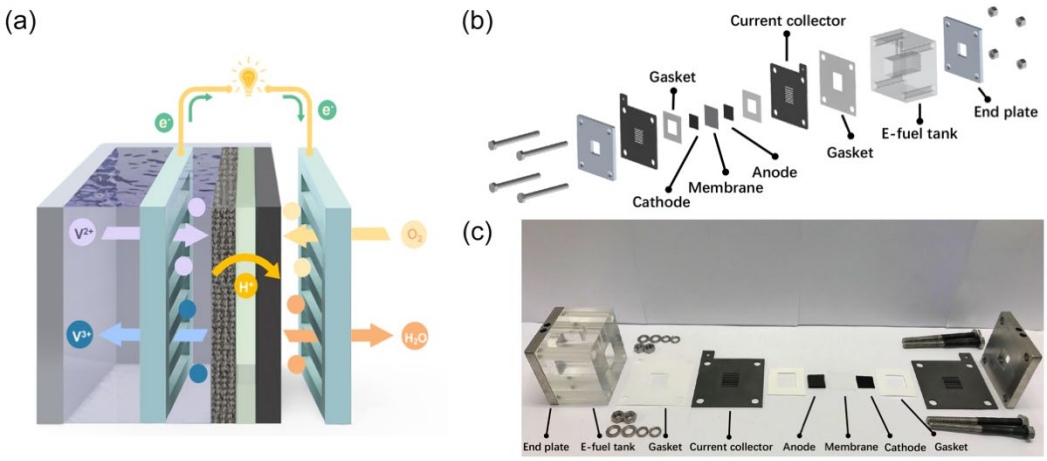

Figure 1 (a) Working principle, (b) design, and (c) fabrication of a passive fuel cell.

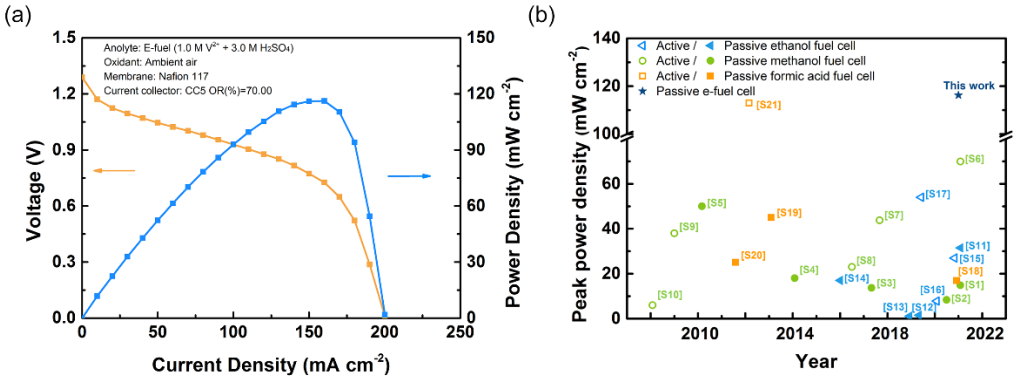

Figure 2 (a) General performance of a passive fuel cell; (b) Comparison of the peak power density of the passive fuel cell with the data available in the open literature.

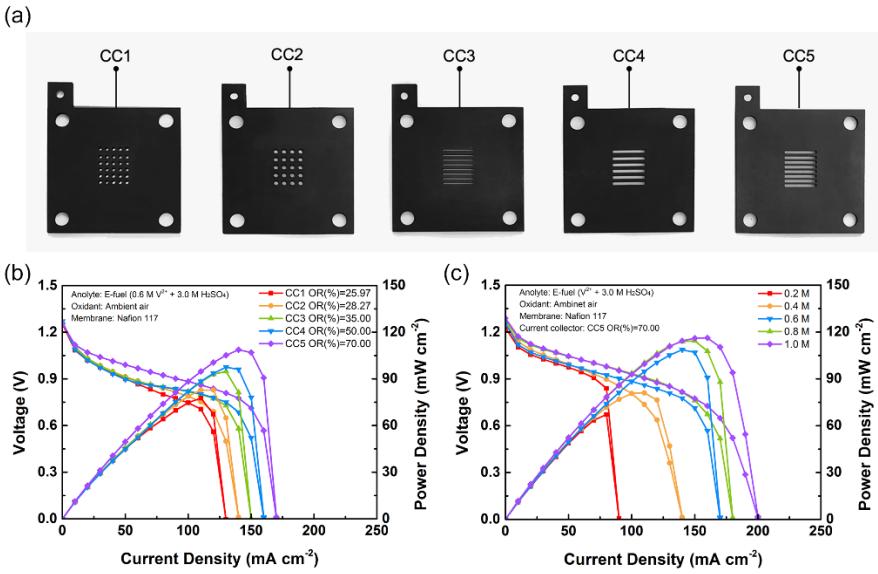

Figure 3 (a) Designs of five current collectors; (b) Polarization and power density curves of this passive fuel cell with different designs; and (c) Polarization and power density curves of this passive fuel cell with various e-fuel concentrations.

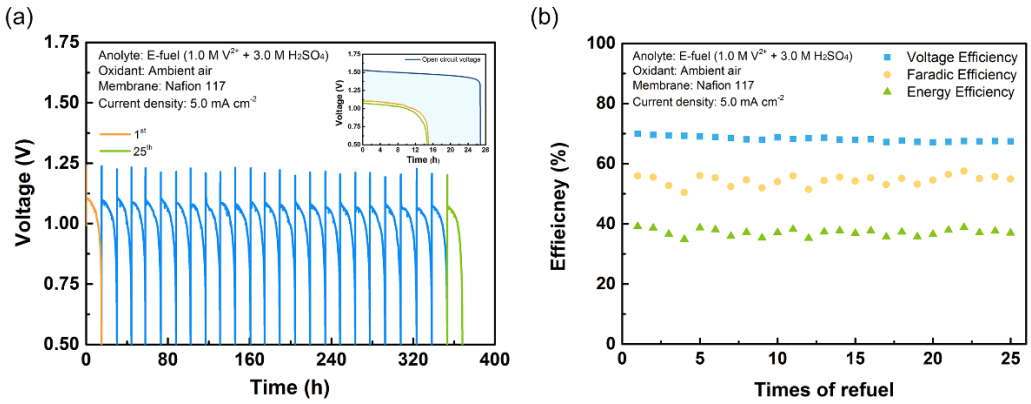

Figure 4 (a) Long-term discharging behavior and comparison of the 1st and 25th discharging curves of this passive fuel cell (insert). (b) The Faradic, voltage, and energy efficiencies of this passive fuel cell.

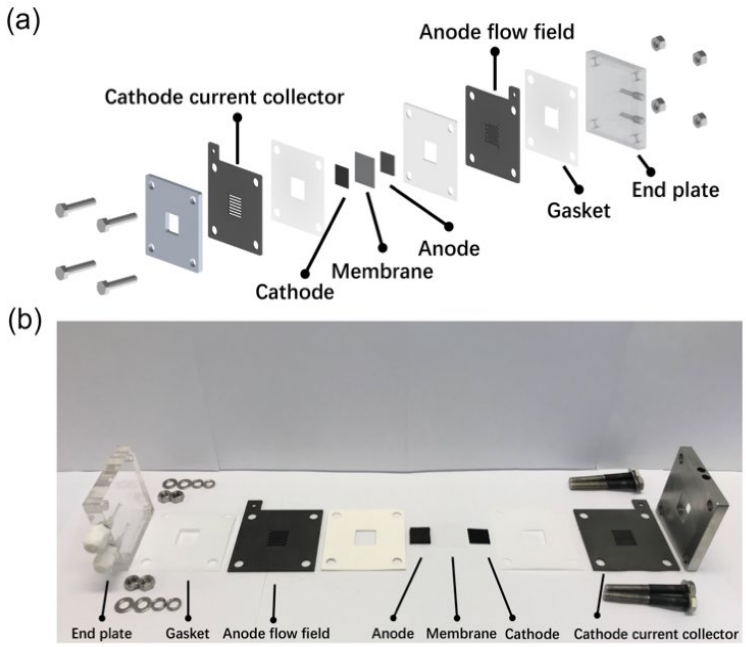

Figure 5 (a) Design and (b) fabrication of a fuel cell with a transparent anode flow field.

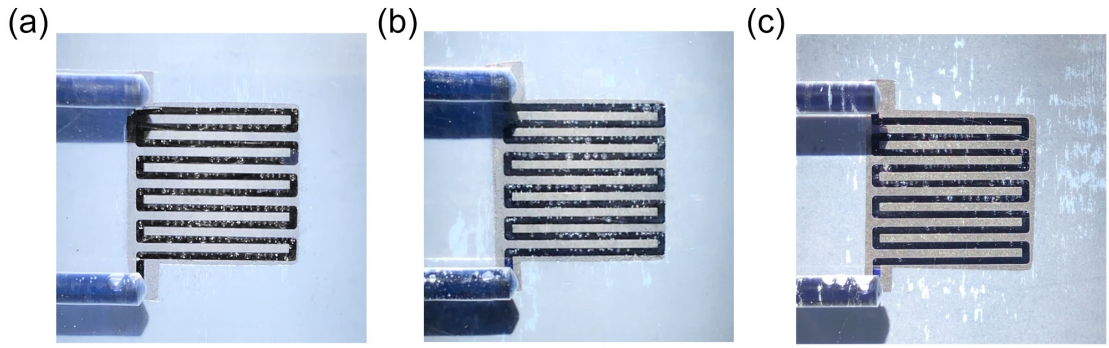

Figure 6 Visualizations of anode flow channels with (a) complete MEA, (b) used and (c) fresh thermally treated graphite felt anode, when fed with e-fuel (1.0 M V^{2+} in 3.0 M H_2SO_4).

Table of Contents (TOC) graphic